Isovector potential of Σ in nuclei and neutron star matter

K. Tsubakihara,[1,2,*] A. Ohnishi,[3] and T. Harada[2]

[1] *Department of Physics, Faculty of Science, Hokkaido University, Sapporo 060-0810, Japan.*
[2] *Department of Engineering Science, Faculty of Engineering, Osaka Electro-Communication University, Neyagawa 060-0810, Japan.*
[3] *Yukawa Institute for Theoretical Physics, Kyoto University, Kyoto 606-8502, Japan.*

(Dated: February 6, 2014)

We determine the coupling constants of Σ hyperon with mesons in relativistic mean field (RMF) models using Σ^- atomic shift data and examine the effects of Σ on the neutron star maximum mass. We find that we need to reduce the vector-isovector meson coupling with Σ ($g_{\rho\Sigma}$) from the value constrained by the $SU(3)_V$ symmetry in order to explain the Σ^- atomic shifts for light symmetric and heavy asymmetric nuclei simultaneously. With the atomic shift fit value of $g_{\rho\Sigma}$, Σ^- can emerge in neutron star matter overcoming the repulsive isoscalar potential for Σ hyperons. Admixture of Σ^- in neutron stars is found to reduce the neutron star maximum mass slightly.

arXiv:1402.0979v1 [nucl-th] 5 Feb 2014

I. INTRODUCTION

Neutron star matter equation of state (NS-EOS) including hyperons is one of the most interesting current subjects in nuclear physics as well as in astrophysics. Hyperons are expected to emerge as the substitutes of nucleons to reduce the Fermi energy in β-equilibrium dense matter, and NS-EOS is strongly affected by the properties of baryon-baryon interactions [1–5]: hyperon-nucleon (YN), hyperon-hyperon (YY) and nucleon-nucleon (NN) interactions. Since hyperon lifetimes are too short to determine YN and YY interactions precisely via scattering experiments, we have to deduce information on these interactions through experimental [6–10] and theoretical [11–14] investigations of hypernuclei which include one or more Λ, Σ and Ξ hyperons. NS-EOSs including hyperons have been proposed so far by taking experimental hypernuclear data into account; they generally predict maximum masses of neutron stars in the range $(1.3-1.7)\ M_\odot$. Recent discoveries of the two-solar-mass neutron stars [15, 16] have cast doubt on these EOSs. The observation is based on the Shapiro-delay, a consequence of the general relativity, and the signal is clearly seen owing to the fortunate inclination angle ($\sin i \sim 1$). From this observation, it is concluded that typical NS-EOSs with hyperons or boson condensates are ruled out. It is a big challenge to construct NS-EOS which is consistent with hypernuclear physics results and supports the two-solar-mass neutron star.

In solving the two-solar-mass NS puzzle mentioned above, there are two key ingredients: constraining YN and YY interactions and understanding the origin of repulsive interactions at high density. Among YN interactions, ΛN interaction is relatively well-known including its spin dependence, and we here concentrate on the ΣN interaction. Since Σ^- is the lightest among the negatively-charged baryons, its appearance is favored in neutron stars because of the charge chemical potential and the nuclear symmetry energy. For example, Glendenning suggested that Σ^- would appear at $(2-3)\rho_0$ in neutron star matter in a relativistic mean field (RMF) framework [17, 18], where Σ potential in nuclear matter was considered to be similar to that of Λ, $U_\Sigma(\rho_0) \sim U_\Lambda(\rho_0) \simeq -30$ MeV. Later on, Σ potential in symmetric nuclear matter is suggested to be repulsive from Σ^- atomic shift data [19], and is confirmed to be repulsive in the quasi-free Σ^- production data [8, 14]. The ΣN repulsion is explained naturally as a consequence of the quark Pauli blocking in quark models [20, 21]. In neutron star matter, Balberg and Gal pointed out that baryon composition is sensitive to the choice of the ΣN interaction [22], and similar conclusions are obtained in RMF approaches [2, 3, 23].

Now it is commonly understood that the isoscalar part of the Σ potential is so repulsive that Σ hyperons tend to be suppressed in NS matter, while we still have ambiguities in the isovector part of the Σ potential. Typical isovector coupling of Σ in RMF is twice that of the nucleons, $g_{\rho\Sigma} \simeq 2g_{\rho N}$, owing to the isospin of Σ, $I_\Sigma = 2I_N = 1$. Atomic shift data of Σ^- atoms, however, suggest much smaller isovector coupling. From the Si and Pb Σ^- atomic shifts, Mares, Friedman, Gal and Jennings obtained the coupling ratio $g_{\rho\Sigma}/g_{\rho N} \simeq 2/3$ [19].

In our previous work, we obtained a further smaller ratio, $g_{\rho\Sigma}/g_{\rho N} = 0.434$, in an RMF model with a logarithmic chiral potential motivated by the strong coupling limit of lattice QCD [24] and $\sigma\zeta$ mixing effects from $U(1)_A$ anomaly [25]. In this RMF model, abbreviated as SCL3, most of the coupling constants have been constrained by the flavor SU(3) ($SU(3)_V$) symmetry for the vector couplings and experimental data of nuclear matter, normal and Λ hypernuclei and Σ atom data. One exception is the ρ-Σ coupling; in order to reproduce atomic shift data of Σ^- atoms, we need to modify $g_{\rho\Sigma}$ from the $SU(3)_V$-constrained value. Smaller $g_{\rho\Sigma}/g_{\rho N}$ ratio leads to a less repulsive potential of Σ^- in neutron star matter, and Σ^- is found to appear in neutron stars even though the isoscalar part of the Σ potential is repulsive. The above conclusion, Σ^- would appear in neutron stars with smaller isovector coupling fitting the atomic shifts,

* tsubaki@oecu.jp

may be model dependent, and should be confirmed with other RMF model parameters.

Another important aspect for the two-solar-mass NS puzzle is the origin of the repulsion at high density. It is well-known that with the non-relativistic effective interaction derived from the bare two-body NN interaction (g-matrix), the saturation point depends on the strength of the tensor interaction and forms a so-called "Coester line", which is off the empirical saturation point. When we include phenomenological three-nucleon repulsion together with the three-body attraction with Δ in the intermediate state, it becomes possible to explain the saturation point and to support two-solar-mass NSs. The above three-nucleon interactions are, however, not enough to support heavy neutron stars, when hyperons are included [26]; the calculated maximum mass of neutron stars with hyperons [26] is less than the precisely measured mass of the Hulse-Taylor pulsar, $1.44M_\odot$ [27]. We need to introduce three-baryon repulsion, which also acts in YNN, YYN and YYY channels [28]. In a relativistic framework, three-body repulsion appears naturally from relativistic kinematics. The attraction from the scalar field appears as the mass reduction, and its effects are relatively smaller at high densities compared with the repulsion from the vector field. As a result, the relativistic Brückner-Hartree-Fock (RBHF) theory can reproduce the saturation point [29], and RMF models generally predict large maximum masses of NSs. This relativistic repulsion could be enough to explain $1.44M_\odot$, but it is not sufficient to describe the newly discovered two-solar-mass NSs when hyperons are taken into account. We need to introduce extra repulsion at high densities also in relativistic frameworks. One of the mechanisms to get extra repulsion in hyperonic matter is to introduce three-baryon interaction [28]. Another way may be to introduce repulsive interaction having different flavor dependence from that adopted in current treatments. The atomic shift fit of Σ^- atoms leads to the modification of hyperon-meson couplings and is related to the second way.

In this article, we revisit Σ hyperons in RMF models and discuss the possibility of Σ^- admixture in neutron star matter. We compare the results of several RMF models with non-linear meson self-energies, where hyperon-meson couplings are determined by reproducing known hypernuclear data. Especially, we examine whether Σ^- should emerge in NS medium when we adopt the parameter sets which can explain the observed Σ^- atomic shifts. Finally, we investigate the maximum mass of NS with NS-EOS constrained by the hypernuclear and exotic atom physics requirements.

II. RELATIVISTIC MEAN FIELD INCLUDING HYPERONS

A. RMF Lagrangian

RMF models are successful in describing various properties of normal nuclei with σ, ω and ρ mesons which couple with nucleons. An RMF Lagrangian for normal nuclei and nuclear matter is given as

$$\begin{aligned}\mathcal{L}_N =& \sum_{i\in N} \bar{\psi}_i \left(i\partial\!\!\!/ - M_i\right)\psi_i + \mathcal{L}_{\sigma\omega\rho} \\ &+ \sum_{i\in N} \bar{\psi}_i \left[g_{\sigma i}\sigma - \gamma_\mu(g_{\omega i}\omega^\mu + g_{\rho i}\boldsymbol{\tau}\cdot\mathbf{R}^\mu)\right]\psi_i \ , \quad (1)\\ \mathcal{L}_{\sigma\omega\rho} =& \frac{1}{2}\,\partial_\mu\sigma\partial^\mu\sigma - \frac{1}{2}\,m_\sigma^2\sigma^2 - V_\sigma\left(\sigma\right) \\ &-\frac{1}{4}\omega_{\mu\nu}\omega^{\mu\nu} + \frac{m_\omega^2}{2}\omega_\mu\omega^\mu + V_\omega\left(\omega\right) \\ &-\frac{1}{4}\mathbf{R}_{\mu\nu}\cdot\mathbf{R}^{\mu\nu} + \frac{m_\rho^2}{2}\mathbf{R}_\mu\cdot\mathbf{R}^\mu \ , \quad (2)\end{aligned}$$

where $V^\mu(V=\omega,\mathbf{R})$ shows the field tensor of the ω or ρ vector mesons, and $\boldsymbol{\tau}$ represents the isospin Pauli matrix. V_σ and V_ω represent σ and ω self-energies,

$$V_\sigma(\sigma) = \frac{1}{3}\,c_{\sigma 3}\sigma^3 + \frac{1}{4}\,c_{\sigma 4}\sigma^4 \ , \quad (3)$$

$$V_\omega(\omega) = \frac{1}{4}\,c_{\omega 4}\left(\omega_\nu\omega^\nu\right)^2 \ . \quad (4)$$

We adopt here NL1 [30], NL-SH [31] and TM1 [32] as typical RMF models for normal nuclei. We also examine the former SCL model (SCL2) [33], where the σ self-energy was derived from analytical calculation in the strong coupling limit of lattice QCD and reads

$$V_\sigma(\sigma) = -\frac{f_\pi^2\left(m_\sigma^2 - m_\pi^2\right)}{2}\left[\log\left(1-\frac{\sigma}{f_\pi}\right) + \frac{\sigma}{f_\pi} + \frac{\sigma^2}{2f_\pi^2}\right] . \quad (5)$$

Their parameter sets are summarized in Table I. We note that coupling constants of these mesons and nucleons are well constrained by fitting binding energies of normal nuclei, while non-linear meson self-energy terms are not determined precisely. While these sophisticated RMF models describe normal nuclear properties well, differences in non-linear terms give rise to large ambiguities in dense matter EOS. Thus it would be possible to discriminate these RMF models for normal nuclei by including hyperons and applying them to NS-EOS.

RMF has been extended to describe also hypernuclei and hyperonic matter [1–5, 25]. A simple extension is to include hyperons in the baryon sum in Eq. (1), $i \in B$, where B represents nucleons (N) and hyperons (Y). It is more natural to include ζ and ϕ, scalar and vector mesons consisting of $\bar{s}s$, respectively, which generate additional attractive and repulsive interactions among hyperons. A

typical RMF Lagrangian including hyperons, ζ and ϕ mesons is given as,

$$\mathcal{L}_B = \sum_{i\in B} \bar{\psi}_i \left(i\partial\!\!\!/ - M_i^* + \gamma_\mu V_i^\mu \right) \psi_i + \mathcal{L}_{\sigma\omega\rho} + \mathcal{L}_{\zeta\phi} \ , \quad (6)$$

$$\mathcal{L}_{\zeta\phi} = \frac{1}{2}\,\partial_\mu\zeta\partial^\mu\zeta - \frac{1}{2}\,m_\zeta^2\zeta^2 - \frac{1}{4}\phi_{\mu\nu}\phi^{\mu\nu} + \frac{m_\phi^2}{2}\phi_\mu\phi^\mu \ , \quad (7)$$

where $\phi^{\mu\nu}$ is the field field tensor for ϕ. The baryon effective masses M_i^* and the vector potentials V_i^μ are given as,

$$M_i^* = M_i + S_i \ , \quad (8)$$

$$S_i = -\left(g_{\sigma i}\sigma + g_{\zeta i}\zeta \right) \ , \quad (9)$$

$$V_i^\mu = g_{\omega i}\omega^\mu + g_{\rho i}\boldsymbol{\tau}\cdot\mathbf{R}^\mu + g_{\phi i}\phi^\mu \ . \quad (10)$$

Here $\boldsymbol{\tau}$ represents the isospin Pauli matrices for $I = 1/2$ baryons (N and Ξ), and the isospin matrices for $I = 1$ (Σ) baryon. In order to keep the normal nuclear properties in the original RMF models, we assume that nucleons do not couple with $\bar{s}s$ mesons and we set $g_{\zeta N} = g_{\phi N} = 0$. This treatment also means that we respect the OZI rule [34], where $\bar{s}s$ does not couple with nucleons, *i.e.,* hair-pin diagrams are suppressed.

TABLE I. The parameters in RMF models, NL1 [30], NL-SH [31], TM1 [32], and SCL2 [33]. The parameters for normal nuclear systems (upper part) are determined in original references. The coupling constants between mesons and hyperons (lower part) are determined in this article based on hypernuclear data. For comparison, we also show parameters in SCL3 RMF model [25] whose meson-hyperon coupling constants have been fixed in the same procedure as this work.

	NL1	NL-SH	TM1	SCL2	SCL3
M_N (MeV)	938	939	938	938	938
m_σ (MeV)	492.250	526.059	511.198	502.63	690
m_ω (MeV)	795.359	783	783	783	783
m_ρ (MeV)	763	763	770	770	770
$g_{\sigma N}$	10.1377	10.444	10.0289	10.08	10.15
$g_{\omega N}$	13.2846	12.945	12.6139	13.02	11.95
$g_{\rho N}$	4.9757	4.383	4.6322	4.40	4.54
$c_{\sigma 3}$ (fm^{-1})	−12.1734	−6.9099	−7.2325	-	-
$c_{\sigma 4}$	−36.2646	−15.8337	0.6183	-	-
$c_{\omega 4}$	0	0	71.3075	200	294.9
m_ζ (MeV)	980	980	980	980	826.3
$g_{\sigma\Lambda}$	6.10	6.405	6.04	6.215	3.40
$g_{\zeta\Lambda}$	6.31	5.85	5.93	5.80	5.17
$g_{\sigma\Sigma}$	4.83	5.13	4.86	4.72	3.16
$g_{\rho\Sigma}$	2.48	1.85	1.87	1.67	1.97

B. Hyperon-Meson Coupling Constants

To examine the neutron star matter properties based on the RMF Lagrangian, Eq. (6), we start from fixing the coupling constants of mesons and hyperons: $g_{\sigma Y}$, $g_{\zeta Y}$, $g_{\omega Y}$, $g_{\rho Y}$, and $g_{\phi Y}$. Unfortunately, it is so time-consuming and sometimes meaningless to vary each coupling constant independently since only their balance can affect the calculated numerical properties. Thus, there are mainly two types of prescriptions to constrain meson-hyperon coupling sets. One of them is based on the picture where we regard the mesons in RMF models are made of $\bar{q}q$. Then the hyperon-meson couplings are constrained by symmetries of quarks. The other is based on the chiral perturbation theory. Scalar and vector fields are generated by the Nambu-Goldstone bosons (pions, kaons, and eta) and low energy coefficients, and σ and ω mesons in RMF are considered to be effective mesons, which represent the scalar and vector fields but are not actual mesons. This picture generally gives smaller σ-hyperon and ω-hyperon couplings compared with the former picture.

Many of RMF models adopt the former picture and assume some symmetry relations in vector meson-baryon coupling constants. For example, some of RMF models employ SU(6) symmetric coupling constants, which corresponds to the naive quark counting. The flavor SU(3) symmetry ($\mathrm{SU(3)_V}$ symmetry) is known to be a better symmetry in hadrons, and constrains the vector meson-baryon interaction Lagrangian as,

$$\begin{aligned}\mathcal{L}_{\mathrm{BV}}^{\mathrm{SU(3)}} &= \sqrt{2}\{g_s\,\mathrm{tr}\left(M_v\right)\mathrm{tr}\left(\bar{B}B\right) + g_D\,\mathrm{tr}\left(\bar{B}\left\{M_v, B\right\}\right) \\ &\quad + g_F\,\mathrm{tr}\left(\bar{B}\left[M_v, B\right]\right)\} \\ &= \sqrt{2}\{g_s\,\mathrm{tr}\left(M_v\right)\mathrm{tr}\left(\bar{B}B\right) + g_1\,\mathrm{tr}\left(\bar{B}M_vB\right) \\ &\quad + g_2\,\mathrm{tr}\left(\bar{B}BM_v\right)\} \ . \end{aligned} \quad (11)$$

Here, B and M_v are flavor SU(3) baryon and vector meson matrices. Under the $\mathrm{SU(3)_V}$ symmetry with the assumption $g_{\phi N} = 0$, all vector meson-hyperon coupling constants are constrained once $g_{\rho N}$ and $g_{\omega N}$ are fixed. From Eq. (11), $\mathrm{SU(3)_V}$ vector coupling constants for Λ and Σ hyperons are given as

$$g_{\omega\Lambda}^{\mathrm{SU(3)}} = \frac{5}{6}g_{\omega N} - \frac{1}{2}g_{\rho N}, \ \ g_{\phi\Lambda}^{\mathrm{SU(3)}} = \frac{\sqrt{2}}{6}\left(g_{\omega N} + 3g_{\rho N}\right) \ , \quad (12)$$

$$g_{\omega\Sigma}^{\mathrm{SU(3)}} = \frac{1}{2}\left(g_{\omega N} + g_{\rho N}\right), \ g_{\phi\Sigma}^{\mathrm{SU(3)}} = \frac{\sqrt{2}}{2}\left(g_{\omega N} - g_{\rho N}\right) \ ,$$
$$g_{\rho\Sigma}^{\mathrm{SU(3)}} = 2g_{\rho N} \ . \quad (13)$$

Naive quark counting also follows the above coupling constant relations. For example, when we set $g_{\rho N} = g_{\omega N}/3$, the above relations lead to the quark counting relation, $g_{\omega\Lambda} = g_{\omega\Sigma} = 2g_{\omega N}/3$. The remaining scalar coupling constants, $g_{\sigma Y}$ and $g_{\zeta Y}$, may be fixed by explaining experimental data of hypernuclear systems.

It should be noted that the above relations are based on the $\bar{q}q$ picture for RMF mesons in the flavor SU(3) limit. If the mesons in RMF contain significant components generated by pions or if the SU(3) breaking effects are strong, hyperon-meson couplings can deviate from

the relation in Eqs. (12) and (13). While it is generally believed that hyperonic EOSs are ruled out by the two solar mass neutron stars [15, 16], the naive quark counting relation mentioned above is respected for ω-hyperon (Λ and Σ) couplings, $g_{\omega Y} \simeq 2g_{\sigma N}/3$, in the ruled-out hyperonic EOS [35]. In the original paper by Glendenning and Moszkowski [35], however, the authors considered other possibilities where heavier neutron star can be supported by hyperonic EOS. Furthermore, additional hyperon-hyperon repulsion coming from the ϕ meson exchange was not considered. Thus we need more care to set the hyperon-meson couplings.

In this work, we adopt flavor $SU(3)_V$ symmetric couplings shown in Eq. (11) as a starting point, and modify some of the coupling constants which have large effects in explaining the hypernuclear data. This procedure enables us to construct NS-EOS which includes hypernuclear information effectively. In the next section, we try to determine the hyperon-meson couplings based on the experimental data.

III. HYPERNUCLEI, EXOTIC ATOMS, AND NEUTRON STARS

In this section, following the procedure adopted in our previous work [25], we introduce Λ and Σ hyperons in the NL1, NL-SH, TM1, and SCL2 RMF models, and fit the Λ separation energies data in single Λ hypernuclei, the $\Lambda\Lambda$ bond energy data in the double Λ hypernucleus, and the Σ^- atomic shifts data. Next we apply the obtained RMF model parameters to calculate the neutron star matter EOS. We can find similar works in the literature, but information of Σ^- atoms were not taken into account and stronger $\Lambda\Lambda$ attraction was assumed in [2], and only one set of the normal nuclear RMF models was used in [19].

A. Lambda Hypernuclei

For Λ hyperon, we have four RMF parameters to be determined: $g_{\sigma\Lambda}$, $g_{\zeta\Lambda}$, $g_{\omega\Lambda}$, and $g_{\phi\Lambda}$. Experimental data of Λ separation energies (S_Λ) in single Λ hypernuclei and the $\Lambda\Lambda$ bond energy ($\Delta B_{\Lambda\Lambda}$) in the double Λ hypernucleus ${}^{6}_{\Lambda\Lambda}$He [7] are available as the constraints of these coupling constants. Unfortunately, the Λ potential at high density is not very sensitive to all of these available data. The baryon potential at low momentum is given as the sum of scalar and vector potentials, $U_B = S_B + V_B^0$, and this potential mainly determines the hypernuclear properties at around normal nuclear density. Both the scalar and vector potentials are approximately proportional to ρ_B at low density, thus we cannot determine the scalar and vector potentials for Λ separately. One may think that additional information on the difference $(S_B - V_B)$ is available from the spin-orbit splitting. However, it is possible to explain the spin-orbit splittings by tuning the tensor coupling of the vector meson, which is not incorporated in the RMF Lagrangian considered in this work. Since the tensor coupling does not affect the EOS of uniform matter in the mean field approximation, the spin-orbit splitting is not helpful to constrain the EOS at high density.

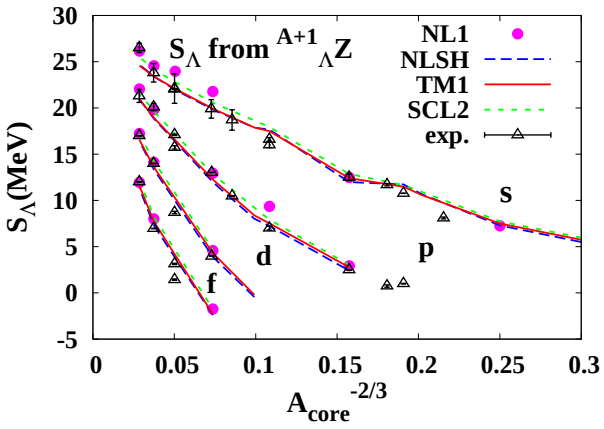

FIG. 1. Experimental and calculated separation energies of Λ from single Λ hypernuclei, S_Λ. Magenta point presents the fitting results based on NL1 RMF model. Broken blue lines presents the fitting results based on NL-SH RMF model. Solid red lines show the fitting results based on TM1 RMF model. Open triangle symbols are experimental S_Λ.

We adopt here the $SU(3)_V$ relations for the vector couplings in Eq. (12), $g_{\omega\Lambda} = g_{\omega\Lambda}^{SU(3)}$ and $g_{\phi\Lambda} = g_{\phi\Lambda}^{SU(3)}$ to fix the vector potentials. The remaining scalar-isoscalar coupling constants, $g_{\sigma\Lambda}$ and $g_{\zeta\Lambda}$, are determined by fitting experimental hypernuclear data: Λ separation energies S_Λ in single Λ hypernuclei and the $\Lambda\Lambda$ bond energy $\Delta B_{\Lambda\Lambda} = 0.67 \pm 0.17$ MeV of the double Λ hypernuclei ${}^{6}_{\Lambda\Lambda}$He observed in the NAGARA event [7, 36].

The obtained coupling constant sets ($g_{\sigma\Lambda}$ and $g_{\zeta\Lambda}$) are summarized in TABLE I. In Fig. 1, we show the calculated results of S_Λ in NL1, NL-SH, TM1 and SCL2 by using the obtained parameter sets as a function of $A_{\rm core}^{-2/3}$, where $A_{\rm core}$ is the mass number of the core nucleus. Since the kinetic energy of Λ is approximately proportional to $1/R^2 \propto A_{\rm core}^{-2/3}$, we can guess the potential depth in nuclear matter as $U_\Lambda \simeq -28$ MeV from the extrapolation to $A \to \infty$ ($A_{\rm core}^{-2/3} \to 0$). We find that experimental S_Λ values are well explained in these RMF models. In addition to the ground state separation energies, excited single particle energies of p, d and f waves are also well described. The Λ shell gaps reflect the strength of the scalar potential via the effective mass M_i^* in Eq. (8), then the scalar potential for Λ seems to have an appropriate strength.

B. Sigma-Nuclear Potential and Σ^- Atoms

For Σ hyperon, we have five RMF parameters, $g_{\sigma\Sigma}$, $g_{\zeta\Sigma}$, $g_{\omega\Sigma}$, $g_{\phi\Sigma}$ and $g_{\rho\Sigma}$. Because of isospin of Σ hyperon, we have one more parameter for the isovector-vector coupling ($g_{\rho\Sigma}$) compared with Λ. Since we have no other knowledge of bound Σ hypernuclei other than ${}^{4}_{\Sigma}$He [37], we have to rely on quasi Σ production reactions [8] and Σ^- atomic shifts data [9].

In Σ^- atoms, a Σ^- moves around a nucleus in the Coulomb orbit. When the Σ^- goes down to small n orbit through subsequent atomic cascade processes (X-ray emission or Auger process), the Σ^- is absorbed in the nucleus via the conversion $\Sigma^- p \to \Lambda n$ inside the nuclei. The X-ray just before the absorption thus contains information of Σ^--nucleus potential. Σ^- atomic shifts have been measured for isospin-symmetric (O, Mg, Al, Si and S) and heavier isospin-asymmetric (W and Pb) nuclei[9]. Once we fix the coupling constants of Σ with isosinglet mesons, Σ^- atomic shift data in heavy nuclei are useful to determine isovector coupling, $g_{\rho\Sigma}$.

We fix the Σ-meson coupling constants in the following way. First, we obtain core nuclear wave functions in RMF. Second, Σ^--nucleus optical potential is given as the Schrödinger-equivalent potential,

$$\mathrm{Re}V_{\mathrm{opt}}^{\Sigma^-} = S_{\Sigma^-}(r) + \frac{EV^0(r)}{M_{\Sigma^-}} + \frac{S^2_{\Sigma^-}(r) - (V^0_{\Sigma^-})^2(r)}{2M_{\Sigma^-}}\ , \tag{14}$$

where S_{Σ^-} and $V^0_{\Sigma^-}$ are the scalar and vector potentials of Σ^- hyperon shown in Eqs. (9) and (10), respectively. Here, the meson fields (σ, ω, ρ) used in S_{Σ^-} and $V^0_{\Sigma^-}$ are those of the core nuclei. Next, we fit the Σ^- atomic shifts for light symmetric nuclei by choosing the isoscalar part of coupling constants properly. Since we do not have ζ and ϕ fields in normal nuclei, atomic shifts have no dependence on $g_{\zeta\Sigma}$ and $g_{\phi\Sigma}$. We adopt SU(3)$_{\mathrm{V}}$ value for $g_{\omega\Sigma}$ and $g_{\phi\Sigma}$, and we invoke naive quark counting for $g_{\zeta\Sigma}$ and assume $g_{\zeta\Sigma} = g_{\sigma\Sigma}/\sqrt{2}$. By tuning $g_{\sigma\Sigma}$, we can well describe Σ^- atomic shifts for light symmetric nuclei.

Finally, we determine $g_{\rho\Sigma}$ by fitting the atomic shifts of heavier Σ^- atoms. In Ref. [25], we found that it is difficult to explain the Σ^- atomic shifts with heavier core-nuclei which is isospin-asymmetric, if we keep SU(3)$_{\mathrm{V}}$ symmetry relation shown in Eq. (11). Thus, we need to modify $g_{\rho\Sigma}$ to reproduce Σ^- atomic shift data in the same way as Ref. [25]. One of the reasons to modify $g_{\rho\Sigma}$ from the SU(3)$_{\mathrm{V}}$ value may be that the isovector part of Σ interaction should be affected by the quark Pauli principle, which cannot be expressed in the meson exchange potential with SU(3)$_{\mathrm{V}}$ relation.

In Fig. 2, experimental and calculated atomic shifts on several core nuclei are shown as a function of the atomic number of core nuclei. Basic trend of Σ^- atomic shift is reproduced sufficiently well. Determined Σ^--core nuclei optical potentials are shown in Fig. 3 for NL1, NL-SH, and TM1 models. Fixed parameters are summarized in Table I. We refer to these fitted $g_{\rho\Sigma}$s as atomic shift (AS) fit values. Compared to SU(3)$_{\mathrm{V}}$ values, $g_{\rho\Sigma} = g_{\omega\Sigma}$, AS fit values of $g_{\rho\Sigma}$ are strongly reduced. From these results, it seems common to all employed RMF models that Σ^- feels repulsive potential in nuclear medium and its height is in the range of 20 $\sim$ 30MeV, and that a few MeV attractive pockets around nuclear surface are essential to explain experimental Σ^- AS especially on ^{208}Pb.

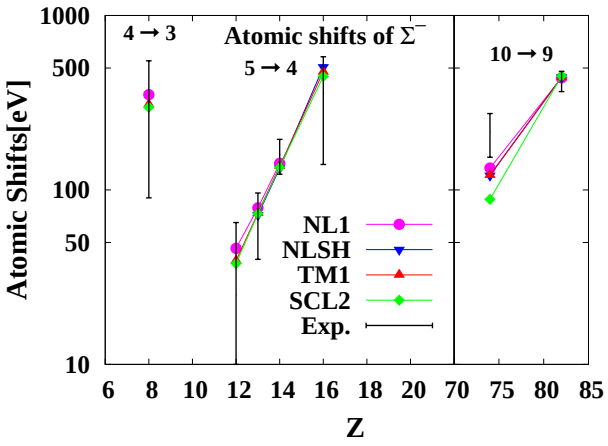

FIG. 2. Experimental and calculated Σ^- atomic shifts as a function of the atomic number of core nuclei. Solid green lines and filled diamonds presents the fitting results based on NL1 RMF model. Solid blue lines and filled inverse triangles presents the fitting results based on NL-SH RMF model. Solid red lines and filled triangles show the fitting results based on TM1 RMF model. Magenta lines are experimental Σ^- atomic shifts on each core nuclei.

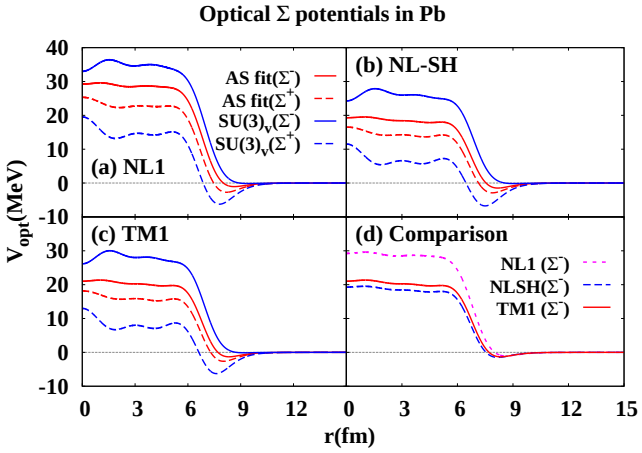

FIG. 3. Schrödinger-equivalent potentials of Σ^- and Σ^+ calculated with (a) NL1, (b)NL-SH, and (c) TM1 RMF models, respectively. The results of parameter sets determined by reproducing Σ^- atomic shift are shown with red lines. The results of parameter sets suggested from SU(3)$_{\mathrm{V}}$ symmetry are presented by blue lines. The real parts of the optical potentials of $\Sigma^-(\Sigma^+)$ are shown by solid(dashed) lines.

In addition to Σ^- optical potentials, we also present Σ^+ potentials in both Σ^- AS fit and SU(3)$_{\rm V}$ cases. By comparing Σ^- and Σ^+ potentials, we can roughly estimate the symmetry energies of Σ and their difference between Σ^- AS fit and SU(3)$_{\rm V}$ cases. The symmetry energies of Σ are reduced from around 15 MeV with SU(3)$_{\rm V}$ values to around 3 MeV with SU(3)$_{\rm V}$ values in all employed RMF models.

C. Neutron Star Matter EOS

Based on the meson-hyperon coupling constants determined in the previous subsection, NS-EOS, for example energy density ($\epsilon = E/V$) and pressure (P) as functions of density, are obtained from the energy–momentum tensor calculated by using RMF Lagrangian, Eq. (6). This procedure enables us to deduce reliable NS-EOS which explains known bulk properties of nuclear and hypernuclear systems. Here, ϵ and P are written as

$$\begin{aligned}\epsilon = T^{00} &= \frac{1}{2}m_\sigma^2\sigma^2 + V_\sigma(\sigma) + \frac{1}{2}m_\zeta^2\zeta^2 \\ &+ \frac{1}{2}m_\omega^2\omega^2 + \frac{3c_{\omega 4}}{4}\omega^4 + \frac{1}{2}m_\rho^2\rho^2 + \frac{1}{2}m_\phi^2\phi^2 \\ &+ \sum_{i=B,l}\frac{\nu_i}{(2\pi)^3}\int_0^{k_F^i} d^3k\sqrt{k^2+(M_i^*)^2}\end{aligned} \tag{15}$$

$$\begin{aligned}P = \frac{1}{3}\sum_i T^{ii} &= -\frac{1}{2}m_\sigma^2\sigma^2 - V_\sigma(\sigma) - \frac{1}{2}m_\zeta^2\zeta^2 \\ &+ \frac{1}{2}m_\omega^2\omega^2 + \frac{c_{\omega 4}}{4}\omega^4 + \frac{1}{2}m_\rho^2\rho^2 + \frac{1}{2}m_\phi^2\phi^2 \\ &+ \sum_{i=B,l}\frac{\nu_i}{(2\pi)^3}\int_0^{k_F^i} d^3k\frac{k^2}{3\sqrt{k^2+(M_i^*)^2}}\end{aligned} \tag{16}$$

In NS matter, the density of each baryons ρ_{Bi} should be determined under the charge neutrality and the β–equilibrium conditions. Thus, the total baryon densities ρ_B, the lepton densities ρ_l, the charge density ρ_c, and the chemical potential μ_{Bi} obey the following equations,

$$\rho_B = \sum_{i=B}\rho_{Bi} \tag{17}$$

$$\rho_{Bi} = \frac{1}{3\pi^2}\left\{(\mu_{Bi}-V_i)^2 - (M_i^*)^2\right\}^{3/2} \tag{18}$$

$$\mu_{Bi} = \mu_B + q_i\mu_c \tag{19}$$

$$\rho_c = \sum_{i=B} q_i\rho_{Bi} + \sum_{j=l}\rho_{lj} = 0 \tag{20}$$

This condition means that all reactions are allowed as long as charge and baryon numbers are conserved. For example, Λ hyperon can emerge as a substitute of n in the high ρ_B region. In this subsection, we examine NS-EOS derived from the RMF models whose coupling constants between mesons and hyperons have been determined in the previous subsection.

In Fig. 4, we compare energy per baryon, $E/A - m_n$, in NS matter in NL1, NL-SH, TM1 and SCL2 parameter sets as a function of baryon density, ρ_B. Compared to TM1 and SCL2, NL1 and NL-SH give us stiffer NS-EOSs. By including the hyperon effects, all of NS-EOSs are significantly softened. In the bottom panel of Fig. 4, we compare the NS-EOSs in several cases in TM1, nucleon (np) matter, $np\Lambda$ matter, and $np\Lambda\Sigma$ matter with SU(3)$_{\rm V}$ and AS fit values of $g_{\rho\Sigma}$. We find that the emergence of Σ^- hyperon softens NS-EOSs further but slightly if we adopt AS fit values of $g_{\rho\Sigma}$. By comparison, the NS-EOSs with SU(3)$_{\rm V}$ values are almost the same as NS-EOSs composed of $np\Lambda$. It is a general trend that NS-EOS suggested by fitting the Σ^- atomic shifts becomes slightly softer than the SU(3)$_{\rm V}$-constrained EOS.

To confirm these results, we examine baryon potentials in NS matter, which are shown in Fig. 5. Compared to SU(3)$_{\rm V}$ cases, it is clear that the Σ^- potentials with AS fit values become less repulsive. This less repulsive Σ^- potential may allow Σ^- hyperon to appear in NS matter with AS fit values and soften NS-EOS.

We show baryon and lepton fractions, $Y_{B,L}$, in NS matter with TM1 for several choices of hyperon effects in Fig. 6. In Figs. 6 (b) and 6 (c), we show calculated baryon and lepton fractions with AS fit and SU(3)$_{\rm V}$ values of $g_{\rho\Sigma}$, respectively. From these results, if we apply AS fit $g_{\rho\Sigma}$, Σ^- tend to appear in NS matter from lower ρ_B compared to that with SU(3)$_{\rm V}$ value. This trend is already suggested in our previous work using SCL3 RMF. Thus, we confirm that it is common to all employed RMF models here and SCL3 RMF model that Λ and Σ^- appear almost simultaneously at around 2-3 ρ_0 if we apply the parameter sets reproducing Σ^- atomic shifts, as shown in Fig. 6 (d).

In Fig. 7(a)-(c), we show calculated NS mass in NL1, NL-SH and TM1 as a function of central baryon density ρ_c, respectively. Maximum masses of hyperonic stars are reduced by including Σ^- in all models. At the same time, NS-EOSs have already been softened strongly by the emergence of Λ hyperon, and the softening effect of Σ^- on NS maximum mass is not very strong. In NL1 and NL-SH, calculated maximum masses of NS exceed $2M_\odot$ even if Λ and Σ hyperons are included, and the recently observed heavy NS [15] can be supported. By comparison, the calculated NS maximum mass in TM1 with hyperons does not reach $2M_\odot$, and the two-solar-mass NS puzzle remains.

It would be premature to conclude that the two-solar-mass NS puzzle can be solved in NL1 and NL-SH RMF models with AS fit values of $g_{\rho\Sigma}$. It seems that the high density region in NS core may be out of the range of applicability in the present treatment of NL1 and NL-SH parameter sets with hyperons; the effective mass of nucleon is reduced too much and it becomes negative at around $4\rho_B$ and $6.5\rho_0$, respectively. The mechanism of the negative nucleon effective mass can be understood as

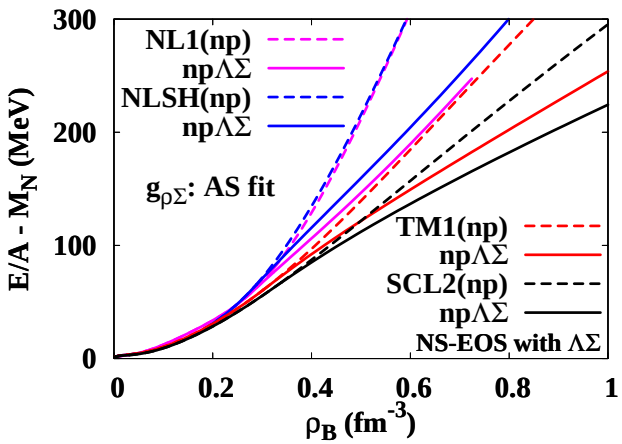

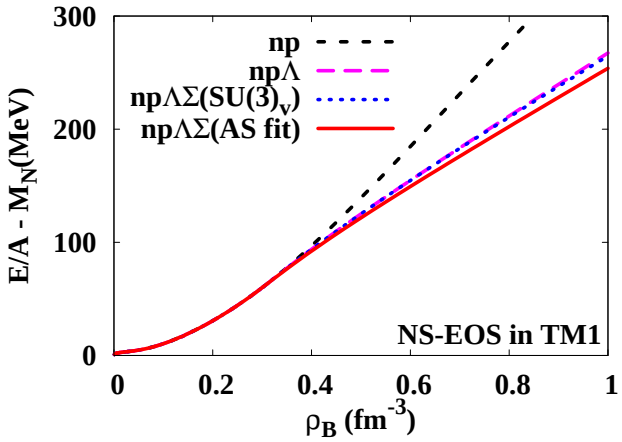

FIG. 4. Calculated NS-EOS based on the RMF models with Λ and Σ hyperons. Upper panel shows NS-EOS in the NL1, NL-SH, TM1 and SCL2 RMF models those coupling constants to hyperons have been determined so as to reproduce Λ and Σ hypernuclear data in this article (AS fit values). Broken lines correspond to NS-EOS with n and p and solid lines represent NS-EOS including Λ and Σ hyperon additionally. Leptons (e and μ) are also considered. In lower panel, we compare NS-EOSs with $SU(3)_V$ and AS fit values in the TM1 RMF model.

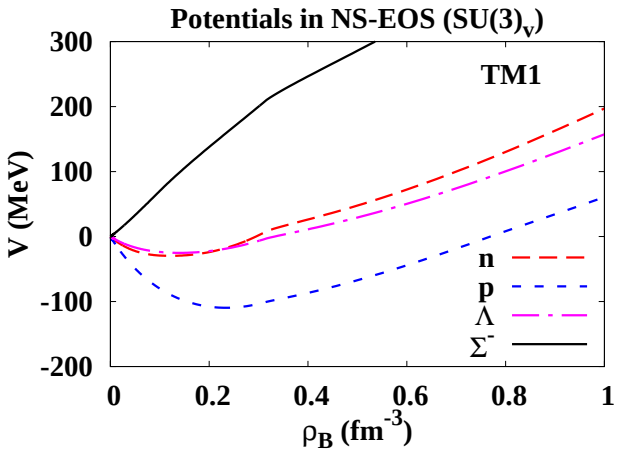

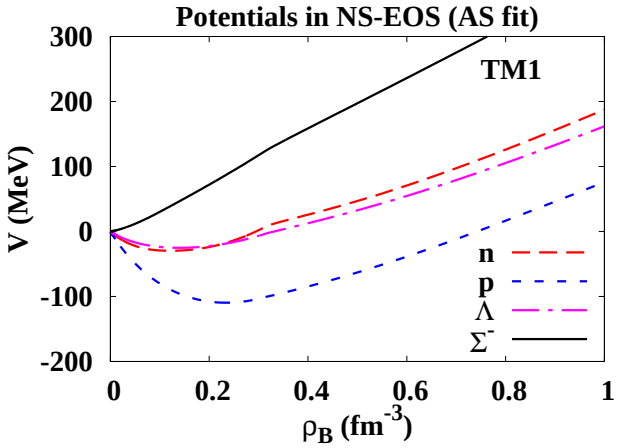

FIG. 5. Calculated potentials of baryons in NS matter on TM1 RMF model. Upper panel shows the results with $SU(3)_V$ $g_{\rho\Sigma}$ values, Eq. (11). Lower panel displays the ones with $g_{\rho\Sigma}$ determined by reproducing Σ^- atomic shifts (AS fit values).

follows. Both nucleons and hyperons act to increase σ as long as their effective mass is positive. At the density where nucleon effective mass vanishes, hyperons are still massive due to the smaller couplings with σ and larger masses in vacuum. These huge mass reductions may correspond to the phase transition from a baryonic matter to a quark matter since they indicate the complete restoration of chiral symmetry.

By comparison, TM1 parameter set is free from the negative nucleon mass problem in the density region considered here, but its maximum mass lies below the observed $1.97M_\odot$; maximum mass of NS in TM1 with hyperons is calculated to be $1.75M_\odot$. In TM1, the ω^4 self-interaction is introduced so as to simulate the scalar and vector potentials in Dirac-Brückner-Hartree-Fock (DBHF) calculation [29]. We have also adopted this ω^4 self-interaction in SCL2 and SCL3 models. The ω^4 term suppresses ω field at high density, and softens the EOS. Then a model with a larger coefficient $c_{\omega 4}$ predict a smaller NS maximum mass. Since NL RMF models do not include ω^4 terms, vector repulsive potentials linearly increase at higher ρ_B as we presented in Fig. 5 of Ref. [25].

Different predictions in the RMF models discussed here implies the importance of three-body interactions [28]. Higher order meson interaction terms such as $\sigma^{3,4}$ and ω^4 may be related to the three-body interactions. These interactions are expected to lead not only re-stiffening effect in EOS but also the suppression to the appearance of hyperons. We introduced explicit three-body couplings to RMF model and examined their effects to high density NS-EOS with preliminary parameter sets which are determined in the same way as we have reported in this work [38]. More detail analysis is strongly needed to give a conclusion of the validity of three-body couplings.

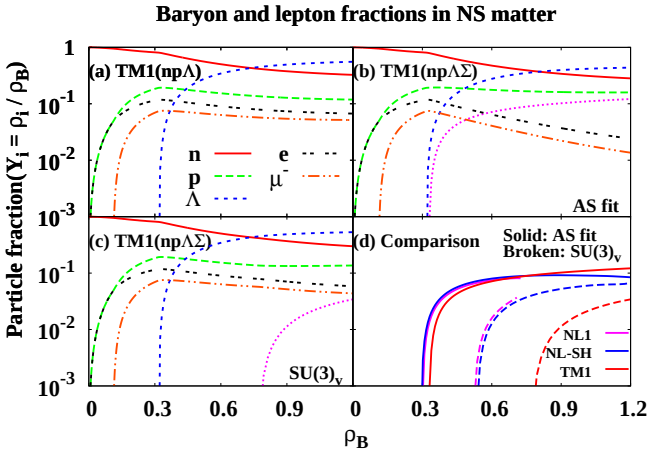

FIG. 6. Baryon and lepton fractions, Y_B and Y_L calculated based on applied RMF model in which hyperon degrees of freedom are introduced. (a) $np\Lambda$ NS matter, (b) $np\Lambda\Sigma$ NS matter ($g_{\rho\Sigma}$: fixed by reproducing the atomic shifts of Σ^-), and (c) $np\Lambda\Sigma$ NS matter ($g_{\rho\Sigma}$: constrained by $SU(3)_V$ symmetric relation) based on TM1 RMF model, respectively; (d) comparison among the results of NL1, NL-SH, and TM1 RMF models.

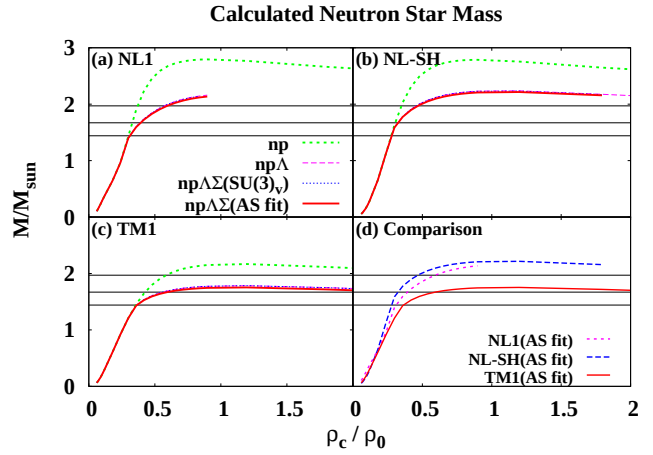

FIG. 7. Calculated NS mass by solving TOV equation based on the RMF model parameters whose meson-hyperon couplings are determined in these references, (a)NL1, (b)NL-SH, and (c) TM1 RMF models, respectively. In panel (d), the comparison among the results of NL1, NL-SH, and TM1 RMF models is presented with green dash line, blue dotted line, and red solid line, respectively.

IV. SUMMARY AND DISCUSSION

In this article, we have investigated neutron star matter equation of state (NS-EOS) based on the RMF models which can reproduce the bulk properties of nuclear systems consisting of nucleons and hypernulcear systems consisting of Λ and Σ hyperons in addition to nucleons. We have emphasized the importance of Σ coupling with isovector-vector (ρ) meson, $g_{\rho\Sigma}$.

The coupling constants of Λ and Σ hyperons in RMF models have been well-constrained by explaining separation energies of Λ (S_Λ) in single Λ hypernuclei, $\Lambda\Lambda$ bond energy ($\Delta B_{\Lambda\Lambda}$) in the double Λ hypernucleus ${}^{6}_{\Lambda\Lambda}$He, and the Σ^- atomic shifts, under the assumption that the isoscalar vector couplings are fixed by the $SU(3)_V$ symmetric coupling constant relations. We have found that we need to reduce $g_{\rho\Sigma}$ from the $SU(3)_V$ value to explain the experimental Σ^- atomic shifts. Then the symmetry energy of Σ in the atomic shift fit case is smaller than that in the $SU(3)_V$ case.

We have examined the hyperon effects on the NS-EOS by using the RMF including hyperons with AS fit and $SU(3)_V$ values of $g_{\rho\Sigma}$. We have confirmed that Σ^- would appear in NS matter with the AS fit $g_{\rho\Sigma}$ value, since the isovector part of Σ^- potential in NS matter is smaller in the AS fit case than in the $SU(3)_V$ case. This trend is common to all of employed RMF parameter sets, NL1, NL-SH, TM1 and SCL2 with AS fit values. Σ^- hyperons can appear in NS matter at $\rho_B \sim 2\rho_0$, which is close to the density where Λ hyperons appear. Thus, it is valuable to revisit the appearance of Σ^- in NS matter, when we want to understand NS based on experimental hypernuclear data including Σ^- atomic shifts.

NS-EOS is softened by Λ and Σ hyperons. The NS maximum mass is reduced by $(0.5-0.6)M_\odot$ when we include Λ, and it is further reduced by including Σ slightly. When we include hyperons in NS-EOS, TM1 RMF model cannot support $2M_\odot$ NS [15, 16], while NL1 and NL-SH could support $2M_\odot$ NS mass. We need more studies to solve the heavy neutron star puzzle conclusively. In NL1 and NL-SH models, nucleon effective mass becomes negative at medium baryon density, and we cannot explain the density dependence of the vector potential obtained in the Dirac-Brückner-Hartree-Fock (DBHF) calculation. In TM1, SCL2, and SCL3 models, ω^4 self-interaction is included to simulate the DBHF results, but these models cannot support the $2M_\odot$ NS.

It was also suggested that Ξ^--nucleus potential is attractive from the analysis about Ξ^- production spectrum [10]. If Ξ hyperons emerge in dense matter, NS-EOS will be softened a little more as in the Σ^- case. We guess, however, that maximum mass will not be affected by inclusion of Ξ^- so much since, as we have shown, NS-EOS has already been softened by including Λ hyperon and Σ^- reduce the electron chemical potential.

From these results, we conclude that re-stiffening mechanisms are required to understand the massive NS properties. As one of candidate to solve this problem, three-body repulsive interactions are suggested to be considered. In Ref. [28], universal three-baryon repulsive interactions were examined. These interactions are expected to lead not only re-stiffening effect but also the suppression to the appearance of Λ, Σ and Ξ hyperons. Thus, further investigation is needed and preliminary re-

sults with explicit three-body couplings in RMF model are reported in Ref. [38]. The detailed analysis is in progress and will be reported elsewhere.

ACKNOWLEDGMENTS

This work was supported in part by the Grants-in-Aid for Scientific Research from JSPS (Nos. (B)23340054 (A. Nakamura(incl. A. Ohnishi)) , (B)23340067 (T. Kunihiro(incl. A. Ohnishi)) , (C)23340271 (A. Ohnishi, K. Morita, T. Kunihiro), and (C)25400278, (T. Harada)), by the Grants-in-Aid for Scientific Research on Innovative Areas from MEXT (No. 2404: 24105001, 24105008), by the Yukawa International Program for Quark-hadron Sciences, and by the Grant-in-Aid for the global COE program "The Next Generation of Physics, Spun from Universality and Emergence" from MEXT.

[1] A. Gal and C. B. Dover, Nucl. Phys. **A585**, 1C (1995).
[2] J. Schaffner and I. N. Mishustin, Phys. Rev. C **53**, 1416 (1996).
[3] C. Ishizuka, A. Ohnishi, K. Tsubakihara, K. Sumiyoshi and S. Yamada, J. Phys. G **35**, 085201 (2008).
[4] N. K. Glendenning and J. Schaffner-Bielich, Phys. Rev. C **58**, 1298 (1998).
[5] I. Bednarek and R. Manka, J. Phys. G **31**, 1009 (2005).
[6] R. E. Chrien [BNL (PI+, K+) COLLABORATION Collaboration], Nucl. Phys. **A478**, 705C (1988); P. H. Pile *et al.*, Phys. Rev. Lett. **66**, 2585 (1991); T. Hasegawa *et al.*, Phys. Rev. C **53**, 1210 (1996); O. Hashimoto and H. Tamura, Prog. Part. Nucl. Phys. **57**, 564 (2006).
[7] H. Takahashi *et al.*, Phys. Rev. Lett. **87**, 212502 (2001).
[8] H. Noumi *et al.*, Phys. Rev. Lett. **89**, 072301 (2002) [Erratum-ibid. **90**, 049902 (2003)]; P. K. Saha *et al.*, Phys. Rev. C **70**, 044613 (2004);
[9] C. J. Batty *et al.*, Phys. Lett. B **74** (1978) 27; R. J. Powers *et al.*, Phys. Rev. C **47**, 1263 (1993).
[10] S. Aoki *et al.*, Phys. Lett. B **355**, 45 (1995); T. Fukuda *et al.* [E224 Collaboration], Phys. Rev. C **58**, 1306 (1998); P. Khaustov *et al.* [AGS E885 Collaboration], Phys. Rev. C **61**, 054603 (2000);
[11] C. B. Dover and A. Gal, Prog. Part. Nucl. Phys. **12**, 171 (1985).
[12] D. J. Millener, C. B. Dover and A. Gal, Phys. Rev. C **38**, 2700 (1988).
[13] H. Bando, T. Motoba and J. Zofka, Int. J. Mod. Phys. A **5** (1990) 4021.
[14] T. Harada and Y. Hirabayashi, Nucl. Phys. A **759**, 143 (2005); T. Harada and Y. Hirabayashi, Nucl. Phys. A **767**, 206 (2006); M. Kohno, Y. Fujiwara, Y. Watanabe, K. Ogata and M. Kawai, Prog. Theor. Phys. **112**, 895 (2004); M. Kohno, Y. Fujiwara, Y. Watanabe, K. Ogata and M. Kawai, Phys. Rev. C **74**, 064613 (2006).
[15] P. B. Demorest *et al.,* Nature **467**, 1081 (2010).
[16] J. Antoniadis *et al.*, Science **340**, 448 (2013).
[17] N. K. Glendenning, Phys. Lett. B **114**, 392 (1982).
[18] B. D. Serot and J. D. Walecka, Adv. in Nucl. Phys. **16** (1986), 1.
[19] J. Mares, E. Friedman, A. Gal and B. K. Jennings, Nucl. Phys. A **594**, 311 (1995) [nucl-th/9505003].
[20] M. Oka, K. Shimizu and K. Yazaki, Nucl. Phys. A **464**, 700 (1987).
[21] Y. Fujiwara, T. Fujita, M. Kohno, C. Nakamoto and Y. Suzuki, Phys. Rev. C **65**, 014002 (2002); Y. Fujiwara, M. Kohno, C. Nakamoto and Y. Suzuki, Phys. Rev. C **64**, 054001 (2001) [nucl-th/0106052].
[22] S. Balberg and A. Gal, Nucl. Phys. A **625**, 435 (1997) [nucl-th/9704013].
[23] P. K. Sahu and A. Ohnishi, Nucl. Phys. A **691**, 439 (2001).
[24] N. Kawamoto and J. Smit, Nucl. Phys. B **190**, (1981) 100; N. Kawamoto, K. Miura, A. Ohnishi and T. Ohnuma, Phys. Rev. D **75**, (2007) 014502 [arXiv:hep-lat/0512023].
[25] K. Tsubakihara, H. Maekawa, H. Matsumiya and A. Ohnishi, Phys. Rev. C **81**, 065206 (2010) [arXiv:0909.5058 [nucl-th]].
[26] M. Baldo, G. F. Burgio and H. J. Schulze, Phys. Rev. C **61**, 055801 (2000) [nucl-th/9912066].
[27] R. A. Hulse and J. H. Taylor, Astrophys. J. **195**, L51 (1975).
[28] S. Nishizaki, T. Takatsuka and Y. Yamamoto, Prog. Theor. Phys. **108**, 703 (2002).
[29] R. Brockmann and R. Machleidt, Phys. Rev. C **42**, 1965 (1990); R. Brockmann and H. Toki, Phys. Rev. Lett. **68**, 3408 (1992).
[30] P.-G. Rheihard *et al.*, Z. Phys. A**323**, 13 (1986).
[31] M. M. Sharma, M. A. Nagarajan and P. Ring, Phys. Lett. B **311**, 377 (1993).
[32] Y. Sugahara and H. Toki, Nucl. Phys. A **579**, 557 (1994).
[33] K. Tsubakihara and A. Ohnishi, Prog. Theor. Phys. **117**, 903 (2007) [nucl-th/0607046].
[34] S. Okubo, Phys. Lett. **5**, (1963) 1975; G. Zweig, *Developments in the Quark Theory of Hadrons* (Hadronic Press, Massachusetts, 1980); J. Iizuka, Prog. Theor. Phys. Suppl. **37**, (1966) 38.
[35] N. K. Glendenning and S. A. Moszkowski, Phys. Rev. Lett. **67**, 2414 (1991).
[36] H. Tamura, private communication.
[37] T. Harada, Y. Akaishi, S. Shinmura and H. Tanaka, Nucl. Phys. A **507**, 715 (1990).
[38] K. Tsubakihara and A. Ohnishi, Nucl. Phys. A **914**, 438 (2013) [arXiv:1211.7208 [nucl-th]].